Ferredoxin III of *Desulfovibrio africanus*: sequencing of the native gene and characterization of a histidine-tagged form

Johanneke L. H. BUSCH*, Jacques L. BRETON*, Sharon L. DAVY*, Richard JAMES†, Geoffrey R. MOORE*, Fraser A. ARMSTRONG‡ and Andrew J. THOMSON*[1]

*Centre for Metalloprotein Spectroscopy and Biology, School of Chemical Sciences, University of East Anglia, Norwich NR4 7TJ, U.K., †Centre for Metalloprotein Spectroscopy and Biology, School of Biological Sciences, University of East Anglia, Norwich NR4 7TJ, U.K., and ‡Inorganic Chemistry Laboratory, Oxford University, South Parks Road, Oxford OX1 3QR, U.K.

Desulfovibrio africanus ferredoxin III (*Da* FdIII) contains one $[4Fe\text{-}4S]^{2+/1+}$ cluster and one $[3Fe\text{-}4S]^{1+/0}$ cluster, bound by seven Cys residues, in which the [3Fe-4S] cluster is co-ordinated by the unusual sequence, Cys^{11}-Xaa-Xaa-Asp^{14}-Xaa-Xaa-Cys^{17}-Xaa_n-Cys^{51}-Glu. The [3Fe-4S] core of this ferredoxin is so far unique in showing rapid bi-directional [3Fe-4S] ↔ [4Fe-4S] cluster interconversion with a wide range of metal ions. In order to obtain protein for mutagenesis studies *Da* FdIII has been cloned, sequenced, and expressed as a hexa-histidine tagged (ht) polypeptide in *Escherichia coli* strain BL21(DE3) pLysS. Expression of ht *Da* FdIII, whether translated from a synthetic gene (pJB10) or from the native nucleotide sequence (pJB11), occurred at similar levels (approx. 6 $mg \cdot l^{-1}$), but without incorporation of metal clusters. The nucleotide sequence confirms the protein sequence reported previously [Bovier-Lapierre, Bruschi, Bonicel and Hatchikian (1987) Biochim. Biophys. Acta **913**, 20–26]. Cluster incorporation was achieved using $FeCl_3$ together with cysteine sulphur transferase, NifS, plus cysteine to generate low levels of sulphide ions. Absorption and EPR spectroscopy show that both [3Fe-4S] and [4Fe-4S] clusters are correctly inserted. Thin-film electrochemistry provides evidence that the [3Fe-4S] cluster undergoes reversible cluster transformation in the presence of Fe(II) and Zn(II) ions with properties identical to the native protein. Nevertheless the protein has lower stability than native *Da* FdIII during chromatography. The one-dimensional 600 MHz NMR spectrum of the apoprotein indicates an unstructured protein with random coil chemical shifts whereas spectra of the reconstituted ht protein show secondary structural elements and 18 peaks shifted downfield of 9.6 p.p.m. The spectra are unique but have similarities with the shift patterns seen with 7Fe *Desulfurolobus ambivalens* Fd. The ht does not affect iron-sulphur cluster incorporation, but NMR evidence suggests that excess Fe binds to the tag. This may account for the lower stability of the ht compared with the native protein.

Key words: iron-sulphur cluster, NifS, site-directed mutagenesis, stability, reconstitution.

INTRODUCTION

Desulfovibrio africanus ferredoxin III (*Da* FdIII), which has 61 amino-acid residues and an M_r 6585, contains one $[4Fe\text{-}4S]^{2+/1+}$ cluster and one $[3Fe\text{-}4S]^{1+/0}$ cluster, bound by seven cysteine residues [1–3]. The [4Fe-4S] cluster is co-ordinated by Cys^{41}, Cys^{44} and Cys^{47} plus the remote Cys^{21}, which is followed by a proline residue. This is a typical [4Fe-4S]-cluster-binding or ferredoxin (Fd) motif [4]. The [3Fe-4S] cluster is co-ordinated by the remaining cysteine residues, Cys^{11}-Xaa-Xaa-Asp^{14}-Xaa-Xaa-Cys^{17}-Xaa_n-Cys^{51}-Glu, where Asp^{14} replaces the more usual Cys and Glu^{52} rather than a Pro follows the remote Cys^{51}. This latter feature has only been observed in one other case, the closely related FdI from *D. vulgaris* (Miyazaki) [5]. The $Cys^{14} \rightarrow Asp$ variation occurs somewhat more frequently, for example, in [3Fe-4S]-cluster-containing Fds from *Pyrococcus furiosus*, *Bacillus schlegelii*, *Sulfolobus acidocaldarius*, *Thermoplasma acidophilum* and *Desulfurolobus ambivalens* [6–10]. [3Fe-4S] clusters can react with metal ions (M)s to produce heterometal cubane clusters $[M:3Fe\text{-}4S]^{2+/1+}$, but the ease and readiness with which this occurs varies widely between proteins. Facile and bi-directional cluster interconversion of the [3Fe-4S] core in *Da* FdIII has been demonstrated for M = Fe(II), Zn(II), Cd(II), Tl(I), Cu(I), Co(II) and Pb(II), using both spectroscopic studies and direct electrochemical methods [3,11,12]. When *Da* FdIII is adsorbed as a film on a pyrolytic graphite edge (PGE) electrode, it is capable of responding rapidly to changes in solution conditions and displays facile cluster conversion. This suggests strongly that the transformations occurring in this particular protein reflect intrinsic properties of the cluster species, rather than extrinsic (protein-structure-based) factors such as steric hindrance or inappropriate positioning of its ligand(s) [12]. In *Da* FdIII the product of the reaction of the $[3Fe\text{-}4S]^{1+}$ core with Fe(II) is a $[4Fe\text{-}4S]^{2+/1+}$ cluster, with a reduced form which has an unusual electronic ground state with spin $S = 3/2$. For most $[4Fe\text{-}4S]^{1+}$ clusters co-ordinated by four thiols in proteins the spin $S = 1/2$ ground state is observed. Such electronic differences may reflect subtle alterations in the co-ordination of the cluster [13,14]. Metal uptake reactions have also been established in *Desulfovibrio gigas* FdII and *P. furiosus* Fd [15–18], but the reaction takes place more rapidly in *Da* FdIII.

Spectroscopic and electrochemical studies of *Da* FdIII and its mixed-metal species have been hindered by the small amounts of native protein available; therefore we expressed *Da* FdIII in

Abbreviations used: *Da* FdIII, *Desulfovibrio africanus* ferredoxin III; Fd, ferredoxin; ht, hexa-His tagged; IPTG, isopropyl-β-D-thiogalactopyranoside; M, metal ion; NifS, cysteine sulphur transferase; PGE, pyrolytic graphite edge; RBS, ribosome binding site; rec *Da* FdIII, recombinant *Da* FdIII; 1D, one-dimensional; 2D, two-dimensional.

The nucleotide sequence data reported will appear in DDBJ, EMBL and GenBank Nucleotide Sequence Databases under the accession number AF208391.

[1] To whom correspondence should be addressed (e-mail a.thomson@uea.ac.uk).

Escherichia coli. Since the nucleotide sequence of the *Da* FdIII gene was unknown, a synthetic gene was synthesized [19] based on the amino-acid sequence of *Da* FdIII [1] and the codon preference for *E. coli* [20]. However, although the *Da* FdIII polypeptide was produced, the iron-sulphur clusters were not inserted *in vivo* [19]. An *in vitro* reconstitution method was therefore developed to achieve cluster insertion into the polypeptide. With this method recombinant *Da* FdIII (rec *Da* FdIII) was obtained with one [3Fe-4S] and one [4Fe-4S] cluster similar to the native protein, as judged by a comparison of EPR, magnetic CD and electrochemical properties [19]. However, rec *Da* FdIII proved to be significantly less stable than the native Fd, raising the question of whether an amino acid sequencing error had arisen or whether mis-folding was taking place. Because insufficient amounts of *Da* FdIII were available to redetermine the amino-acid sequence, we cloned and sequenced the native *Da* FdIII gene. This is reported in the present paper together with the expression, purification, cluster incorporation and characterization of the hexa-His-tagged (ht) FdIII.

MATERIALS AND METHODS

Plasmids, bacterial strains and media

E. coli strain JM83 was grown aerobically at 37 °C in Luria–Bertani ('LB') medium [21], supplemented where required with ampicillin (100 $\mu g \cdot ml^{-1}$). The plasmid pUC18-*Sma*I/BAP was purchased from Pharmacia Biotech (Milton Keynes, U.K). A 40-l culture of *D. africanus* strain Benghazi (NCIMB 8401), which was donated by Dr. E. Claude Hatchikian (Centre National de la Recherche Scientifique, Marseille, France), was grown according to published methods [22], producing 15 g of cell paste, All reagents were of the highest available analytical grade.

DNA manipulation

Genomic DNA was isolated from 3 g of *D. africanus* cells following standard methods [23]. Digestion with restriction enzymes (Boehringer Mannheim GmbH), agarose gel electrophoresis, ligation with T4 DNA ligase (New England Biolabs, Beverly, MA, U.S.A) and transformation were performed essentially as described by Sambrook et al. [21] and in accordance with the instructions of the supplier. DNA was purified from ultra-pure agarose gels (Gibco BRL) using either the Geneclean II kit (Bio 101, Vista, CA, U.S.A.) or the Qiaex II kit (Qiagen Inc., Chatsworth, CA, U.S.A.). For routine analysis of plasmids the Insta-Prep kit (3′ → 5′, Boulder, CO, U.S.A.) was used. DNA for sequencing was purified with the Qiagen Plasmid kit (Qiagen). [α-^{32}P]dCTP, Multiprime DNA Labelling System, and Hybond-N^+ membranes were obtained from Amersham. Radioactively labelled oligomers were purified on Nick columns (Pharmacia). DNA concentrations were estimated with the Gene Quant from Pharmacia. Synthetic oligonucleotides were made in the University of East Anglia oligonucleotide synthesis facilities.

DNA sequencing

DNA sequencing was carried out on the A.L.F. DNA sequencer (Pharmacia–LKB). The sequencing reactions were performed with the AutoRead Sequencing Kit (Pharmacia), according to the manufacturer's recommendations. Blast searches of DNA sequence databases were performed via the internet.

Construction of expression vectors for ht *Da* FdIII

Plasmid pJB10, comprising the *Da FdIII* gene with a C-terminal ht extension, was prepared by cloning the synthetic *Da FdIII* gene into the pET21d vector. Primer H31 (5′-GCATCCATGG GTTACAAAATCACC-3′) was constructed to introduce an *Nco*I restriction site (underlined) around the start codon of the *Da FdIII* gene. Primer L60 (3′-CGCGACTGGCAACTTCTT-TTGGAGCTCG-5′) was used to introduce a downstream *Xho*I site to replace the stop codon of the *Da FdIII* gene. Flanking *Nco*I and *Xho*I restriction sites enable the directional cloning of the *Da FdIII* gene into pET21d and the introduction of the ht at the C-terminus of the *Da* FdIII protein. The resulting plasmid (pJB10) was transformed into *E. coli* BL21(DE3) pLysS. Plasmid pLysS expresses small amounts of T7 lysozyme, which inhibits transcription before induction with isopropyl-β-D-thiogalactopyranoside (IPTG) [24].

Plasmid pJB11 was constructed using the same procedure as for the preparation of pJB10. However, instead of using the synthetic gene of *Da FdIII* as the DNA template, PCR reactions were carried out with the native *Da FdIII* nucleotide sequence as the DNA template (plasmid pJB2, see the Results section). Thus two plasmids were constructed which encoded the *Da FdIII* gene, with a different codon usage, namely *E. coli* preference and native *D. africanus* codon usage, to compare protein expression levels from the two plasmids.

Expression of ht *Da* FdIII

E. coli BL21(DE3) pLysS strain transformed with plasmid pJB10 was grown at 37 °C in 5 l of Luria–Bertani medium, in 2-l baffled flasks, each containing 500 ml. The medium was supplemented with 0.7 mM ampicillin (Beecham Research, Welwyn Garden City, U.K.) and 34 $\mu g \cdot ml^{-1}$ chloramphenicol. Induction with 1 mM IPTG (Melford Laboratories, Ipswich, U.K.) was performed when the attenuance (D_{600}) of the culture had reached 0.6. Harvesting by centrifugation was carried out after 2.5–3 h of protein expression ($D_{600} = 1.6$). 12 g of wet-weight cells were collected from 5 l of cultures and stored at −80 °C. Samples, before induction and harvesting, were subjected to SDS/PAGE in a Bio-Rad Mini-Protean II vertical slab-gel unit, following a procedure adapted from Laemmli [25].

Purification

Approx. 12 g of cell paste from a 5-l shake-flask culture of BL21(DE3) pLysS bearing the ht *Da* FdIII-expressing plasmid pJB10 was thawed in 50 ml of binding buffer (20 mM Tris/HCl, pH 7.9, 500 mM NaCl, 5 mM imidazole); protease inhibitors (1 mM PMSF and 1 mM pepstatin), approx. 20 μg of DNase I and RNase A and 100 mg of $MgCl_2.6H_2O$ were added. The cell suspension was treated on a French pressure cell press (SLM Aminco) at a maximum external pressure of 7 MPa (several passages) and lysed cells were centrifuged at 170000 ***g*** for 90 min at 4 °C, yielding a clear supernatant. An affinity column (1 cm diam., 7.5 ml volume) of Ni-IDA (iminodiacetic acid) Sepharose (His-Bind from Novagen, Madison, WI, U.S.A.) was prepared and eluted according to the manufacturer's recommendations. The column was washed with AnalaR water (3 column vol.), loaded with charge buffer (50 mM $NiSO_4$, 5 column vol.), followed by binding buffer (3 column vol.). The nickel-charged column was loaded with the clear supernatant at 0.8 $ml \cdot min^{-1}$, washed with binding buffer (10 column vol.) and wash buffer (20 mM Tris, pH 7.9, 500 mM NaCl, 60 mM imidazole; 6 column vol.), followed by 6 column vol. of 100 mM imidazole in buffer (20 mM Tris/HCl, pH 7.9, 500 mM NaCl) and a further 6 column vol. each of 150 mM and 200 mM imidazole in buffer. Collected fractions of approx. 5 ml were analysed by SDS/PAGE and the purest fractions were pooled, yielding a 180-ml solution,

consisting mainly of ht *Da* FdIII and a larger molecular mass protein contamination ($\approx$ 30000 Da). The volume of this solution was reduced by precipitation with ammonium sulfate (0–80 % saturation) at 0 °C and centrifuged at 16000 ***g*** for 30 min. The resulting white precipitate was resuspended in 25 ml of 50 mM Tris/HCl, pH 7.6, 2 mM DTT, dialysed (1 cm diam., 3500 Da molecular-mass cut off dialysis tubing) against the same buffer and concentrated in an 8 MC Amicon cell equipped with a YM3 membrane. One third (1.8 ml) of the concentrated, dialysed solution in 50 mM Tris/HCl, pH 7.6, 100 mM NaCl, 10 mM DTT was applied to a Sephacryl S-100 column (2 cm diam. $\times$ 100 cm, Pharmacia), equilibrated and eluted with the same buffer at a flow rate of 0.7 ml$\cdot$min^{-1}. The absorption at 280 nm of the eluate was monitored and 5-ml fractions were collected. Fractions were analysed by SDS/PAGE, which showed that the 30000 Da protein had eluted prior to the ht *Da* FdIII protein. Pure ht *Da* FdIII fractions were pooled and concentrated in an 8 MC Amicon cell fitted with a YM3 membrane. The other fractions were dialysed, and concentrated ht *Da* FdIII-containing solution was applied to the re-equilibrated S-100 column in two batches. Pure ht *Da* FdIII fractions, as judged by SDS/PAGE, were pooled and concentrated in the Amicon unit (YM3 membrane).

Reconstitution

The sulphur transferase (NifS) converts L-cysteine to sulphur and alanine [26] with a slow release of sulphur. The NifS-expressing plasmid pDB551, donated by Dr. Dennis R. Dean (Virginia Polytechnic Institute, Blacksburg, Virginia, U.S.A.) was used to overexpress NifS in *E. coli*. NifS was purified according to published methods [26]. The reconstitution reaction of ht *Da* FdIII in the presence of NifS was adapted from the procedure of Zheng et al. [26]. Reconstitution and further protein treatment were carried out in an anaerobic glovebox (Faircrest, Croydon, UK) operating under an N_2 atmosphere with $O_2 < 1$ p.p.m., monitored with a Systech EC 90 oxygen meter (Systech Instruments, Ltd., Thame, Oxfordshire, U.K.). The following stock solutions were prepared in 50 mM Tris/HCl, pH 8.3, unless otherwise stated; 50 mM DTT, 50 mM L-cysteine and 50 mM ferrous ammonium sulphate (freshly prepared in AnalaR water). Reconstitution reactions were carried out in 2.5-ml aliquots. Reconstitution mixtures contained approx. 70 μM apo-(ht *Da* FdIII), 1.5 mM DTT, 0.6 mM L-cysteine, 1.2 mM ferrous ammonium sulphate and approx. 1 μM NifS, and were incubated overnight.

To remove excess reagents from the reconstitution mixtures, gel-filtration chromatography was applied. A Sephacryl S-100 column (1 cm diam. $\times$ 12 cm) was equilibrated and eluted with 20 mM Hepes, pH 7.4, 100 mM NaCl. To maintain good resolution upon elution, 1.5-ml of reconstitution mixtures were loaded on to the column each time. Eluted brown fractions of high A_{386}/A_{280} ratio were pooled and concentrated in an Amicon 8 MC unit equipped with a YM3 membrane, and further treatment was according to sample requirements. No black precipitation was observed upon S-100 column elution.

Electrospray MS

Electrospray MS was performed on a Fisons VG Platform quadrupole mass spectrometer (Fisons, Beverly, MA, U.S.A.). A Hewlett Packard LC1090 was used as the solvent delivery system. Spectra were analysed with Masslynx, version 2.1 (Fisons VG). The analyser was calibrated with horse heart myoglobin (16951.48 Da). Samples for analysis were prepared by diluting a concentrated protein sample in a suitable solvent, usually 50 % (v/v) acetonitrile in H_2O, containing 0.1 % formic acid. The formic acid was added to aid the formation of positive ions. 20-μl aliquots were injected into the rheodyne port. Typical sample concentrations were 20 pmol$\cdot\mu$l^{-1} (10 μg$\cdot\mu$l^{-1}). The sample was scanned for 100 s and an average scan was produced and analysed.

Spectroscopy

UV/visible absorption spectra were recorded with a Hitachi U-4001 spectrophotometer or a HP845x Diode Array spectrophotometer (Hewlett Packard). Holo ht *Da* FdIII concentrations were determined by using the molar absorption coefficient ϵ = 28.6 mM$^{-1}\cdot$cm^{-1} at 408 nm, as reported for native *Da* FdIII [1].

EPR spectra were recorded on an X-band Bruker ER-200D SRC spectrometer (Karlsruhe, Germany) (perpendicular mode, 9.64 GHz) equipped with an Oxford Instruments ESR-900 helium-flow cryostat and a TE-102 microwave cavity. Field intensity was monitored by a Hall probe and the microwave frequency was measured using a microwave counter from Marconi Instruments (model 2440; Stevenage, Herts., U.K). Data were collected using a dedicated Bruker ESP-1600 computer. Spin densities of paramagnetic samples were estimated from integrations of EPR absorption spectra using 1 mM Cu(II)/10 mM EDTA as the standard solution [27].

^{1}H-NMR spectra were recorded on a Varian Unity Inova 600 spectrometer operating at a ^{1}H frequency of 599.167 MHz. With the exception of the series of one-dimensional (1D) data, which were acquired over the temperature range of 8–25 °C, all spectra were recorded at 15 °C. At this temperature the chemical shifts given were measured from the $^2H_2O/H_2O$ peak at 4.86 p.p.m. and are quoted relative to the methyl resonance of 2,2-dimethyl-2-silapropanesulphonic acid at 0 p.p.m. The spectra were processed with Felix 95 (Biosym Technologies, Inc., San Diego, CA, U.S.A.) running on a Silicon Graphics Indigo 4000 work-station.

1D spectra were acquired over spectral widths of 9–50 kHz with water suppression achieved by presaturation of the $^2H_2O/H_2O$ resonance during the relaxation delay (0.8 s) or by the superWEFT sequence [28]. For holo ht *Da* FdIII the optimum spectra were obtained with a recycle time of 500 ms (relaxation delay + acquisition time) and a time delay of 200 ms. Typically 34000 data points were acquired and Fourier-transformed either without a window function or with a sine-bell squared window function applied prior to transformation. T_1 relaxation times of the fast relaxing peaks were estimated from the null times obtained using the standard inversion-recovery sequence of RD-180°-t-90 °-acq [29]. Twenty spectra with time values ranging from 0–2 s and a recycle time of 2 s were acquired. A recycle time of 2 s was used to ensure the system relaxed back to its equilibrium state between experiments.

Two-dimensional (2D) homonuclear TOCSY [30] and NOESY [31] experiments were acquired using standard sequences. Clean TOCSY experiments [32], with a typical spin-lock field of 12000 Hz (MLEV-17 spin-lock sequence) [33], were recorded with spin-lock durations of 50 and 100 ms. NOESY spectra were recorded with mixing times of 100 and 150 ms with water suppression achieved using the WATERGATE sequence [34]. Spectra were recorded in the phase-sensitive mode using the States-TPPI procedure [35]. All 2D experiments were acquired over a spectral window of 9000 Hz in both dimensions. Typical data sets for 2D homonuclear experiments were 512 increments of 96 transients recorded over 2000 data points. Prior to Fourier transformation an unshifted or shifted (90°) sine-bell squared window function was applied in both the F_1 and F_2 dimensions.

Typically data sets were zero-filled to give a final matrix size of 2000×2000 data points.

Voltammetry

All voltammetry was performed with three-electrode, all-glass cells as described by Armstrong et al. [36]. Measurements were either carried out in an anaerobic glovebox (Belle Technology, Dorset, England) operating under an N_2 atmosphere with $O_2 <$ 2 p.p.m., or on the benchtop with cell anaerobicity maintained by passing a stream of high grade Ar across the solution surface. The PGE working electrode was polished before each experiment using an aqueous alumina slurry (Buehler micropolish, 1.0 μm) and then sonicated extensively to remove traces of Al_2O_3. This was inserted into the main cell compartment which was thermostated at temperatures 0–4 °C. The reference was a saturated calomel reference electrode (SCE) located in a side arm linked to the main compartment by a Luggin tip, and maintained at 22 °C. Potentials were converted to the standard hydrogen electrode (SHE) by using $E_{SCE} = +244$ mV, and values are reported as the means $\pm$ S.E.M. An Eco-Chemie Autolab (Eco-Chemie, Ütrecht, Netherlands) electrochemical analyser was used to obtain most of the data. For protein-film voltammetry, a film of ht *Da* FdIII was obtained by spreading approx. 2 μl of ice-cold protein solution [typically 0.1 mM in buffer containing 0.2 mg/ml polymyxin B sulphate (Sigma) added from a concentrated stock solution] evenly across the surface of a freshly polished PGE electrode. The coated electrode was then transferred to the electrolyte solution and the potential cycled between 0 and -950 mV. After several cycles the voltammetry stabilized to reveal well-defined signals consisting of oxidation and reduction peaks. For bulk solution voltammetry, the protein was typically 0.1 mM in the electrolyte solution which also contained 2 mM neomycin sulfate (Sigma). Polymyxin and neomycin co-adsorb with Fd at the electrode; neomycin binds less tightly than polymyxin and provides a more dynamic film, as required for bulk solution electrochemistry.

RESULTS

Cloning and sequencing of the *Da* FdIII gene

Two degenerate oligonucleotide primers based on the amino-acid sequence of *Da* FdIII were constructed with low redundancy. The iron-sulphur-cluster-binding domains were not included in the primer sequence to prevent possible annealing of the primers to *Da* FdI and *Da* FdII genes. Furthermore, amino-acid residues near the C-terminus were avoided for the primer design, as a possible amino-acid sequencing error for one of these residues was suspected. Primer R5 [5′-TA(C/T)AA(G/A)AT(T/C/A)-AC(A/C/G/T)AT(T/C/A)GA(C/T)AC-3′] was a degenerate 20-mer based on the residues 2–8 and positioned at the N-terminus, and the degenerate 20-mer R6 [3′-CT(C/T)CA-(A/C/G/T)AC(A/G)CT(C/T)GT(C/T)CT(A/G)CG-5′] comprised the residues 49–55 near the C-terminus. Primers R5 and R6 were used in PCR with 2 μg of *D. africanus* genomic DNA as a template, using standard PCR conditions (see the Materials and Methods section). The resulting fragment was purified from an agarose gel with the Qiagen II kit and ligated into the pCR-II vector. The cloned PCR product was sequenced and shown to be part of the *Da FdIII* gene. Two internal restriction sites (*Pst*I and *Hin*cII) were identified in the PCR fragment.

Purified PCR product was labelled with [α-^{32}P]dCTP by the Multiprime DNA Labelling System. Total genomic DNA from *D. africanus* was separately restricted for 16 h with 10 different restriction enzymes, electrophoresed, blotted on to nucleic-acid-transfer membrane (Hybond-N$^+$) and probed with the labelled PCR fragment. The *Eco*RV digestion showed a single band of approx. 650 bp hybridizing to the PCR probe. Fragments of about 650 bp of *D. africanus* genomic DNA, restricted with *Eco*RV, were isolated from an electrophoresed agarose gel, purified with the Geneclean II kit and ligated into the pUC18-*Sma*I/BAP plasmid. Resulting colonies were blotted onto Hybond-N$^+$ membranes and probed with the same labelled PCR fragment as described above. The plasmid hybridizing to the probe was isolated and called plasmid pJB2. Single restrictions with *Pst*I and *Hin*cII confirmed the presence of these internal restriction sites that are found in the *Da FdIII* gene. The plasmid was sequenced with the Universal Reverse primer (Figure 1).

To enable sequencing of the complementary DNA strand of pJB2 two plasmids were constructed (pJB3 and pJB4), each containing one half of the *Da FdIII* gene. pJB3, bearing the upstream half of the *Da FdIII* gene, was obtained by cloning the *Bam*HI/*Hin*cII restricted fragment of pJB2 (approx. 200 bp) into *Bam*HI/*Hin*cII double-digested pUC18. Plasmid pJB4, which comprises the downstream half of the *Da FdIII* gene, was constructed by removal from pJB2 of the approx. 200-bp fragment flanked by *Pst*I restriction sites. The nucleotide sequences of plasmids pJB3 and pJB4 were determined using the Universal Forward sequencing primer.

The nucleotide sequence of the *Da FdIII* fragment cloned into plasmid pJB2 and comprising the *Da FdIII* gene is shown in Figure 1. Comparison of the translated amino-acid sequence with the published amino-acid sequence of *Da* FdIII [1] shows that they are identical. Hence the amino-acid composition of *Da* FdIII is confirmed by the DNA-sequence determination of the cloned native *Da FdIII* gene. Upstream of the gene a ribosome binding site (RBS) was identified (GGAGG) (Figure 1), which has sequence similarity to the RBS of various other *Desulfovibrio* genes, as based on database searches. No potential promoter site for RNA polymerase could be identified upstream of the *Da FdIII* gene in the DNA fragment pJB2. Comparison with other *Desulfovibrio* genes showed that the -35 promoter site is usually found between 40 and 200 bases upstream of the gene (e.g. [37]). Plasmid pJB2 contains only 116 bases upstream of the *Da FdIII* gene. Further downstream of the gene a GC-rich inverted-repeat (IR) stem-loop structure was recognised, which is typical of a transcription terminator signal [38]. This transcription-terminator signal is suggestive of the end of an operon which could account for the lack of a promoter site directly upstream of *Da FdIII* gene in plasmid pJB2. A stop codon was identified upstream of the *Da FdIII* gene at base position 95 and a putative open reading frame for the nucleotide stretch upstream of it is indicated (Figure 1). Database searches of both this nucleotide sequence and the translated protein sequence showed no homology to known proteins.

Expression and purification of ht *Da* FdIII

The expression of ht *Da* FdIII was accomplished in *E. coli* strain BL21(DE3) pLysS transformed with plasmids pJB10 and pJB11 after IPTG induction as shown by SDS/PAGE analysis (Figure 2, upper panel). The expressed protein has a lower mobility than recombinant *Da* FdIII (results not shown), confirming the higher mass of ht *Da* FdIII resulting from the ht extension. Expression of ht *Da* FdIII, whether translated from the synthetic gene (pJB10) or the native nucleotide sequence (pJB11), occurred at similar levels (Figure 2, upper panel), yielding approx. 6 mg·l^{-1} indicating that the codon composition of the *Da FdIII* gene did not significantly influence expression levels.

```
  1 TTGCATGCCTGCAGGTCGACTCTAGAGGATCCC CA TCC TGC CCT GCA ACG GCG          6
            PstI HincII       BamHI

    Trp Thr Ala Gln Gly Lys Tyr His Asn Ala Lys Ser Ser Stop             19
 54 TGG ACC GCA CAG GGC AAG TAT CAT AAC GCA AAG AGT TCG TAG   TAAAATTCC

107 GGAGGTATCATC
     RBS

    Met Gly Tyr Lys Ile Thr Ile Asp Thr Asp Lys Cys Thr Gly Asp Gly Glu  17
117 ATG GGT TAC AAG ATC ACC ATC GAC ACC GAC AAG TGC ACC GGC GAC GGC GAG
                  R5

    Cys Val Asp Val Cys Pro Val Glu Val Tyr Glu Leu Gln Asp Gly Lys Ala  34
168 TGC GTG GAC GTT TGC CCT GTC GAG GTC TAT GAG CTG CAG GAC GGC AAG GCT
                                                PstI

    Val Ala Val Asn Glu Asp Glu Cys Leu Gly Cys Glu Ser Cys Val Glu Val  51
219 GTC GCG GTC AAC GAG GAT GAG TGC CTC GGC TGC GAG TCT TGC GTC GAA GTT
          HincII

    Cys Glu Gln Asp Ala Leu Thr Val Glu Glu Asn Stop                     62
270 TGC GAG CAG GAC GCT CTG ACC GTC GAA GAG AAC TAG TCCAGGTTTCGCCCGATCT
       R6

325 GAAGCGGGAACGGTGGATCTCCACTGTTCCCGCTTTTTTTGTTTGCGTCGGCGCCCGCCATTTCCTT
       IR              IR

392 CGATCCGTTTCCACTTGATCGTCTCCGTTGATTGCCGTCCATTGACGGATCGCCTGATCGCACTTAC

459 TAACTTGAGTCCTGCCGCGACCTAATAGGCGCTTGATGGGCACACGCGCCGACAAG3'
```

Figure 1 Nucleotide sequence of the *Da FdIII* gene and its translated amino-acid sequence

The DNA sequence was determined from plasmids pJB2, pJB3 and pJB4. Locations of the oligonucleotide primers R5 and R6 are shown by arrows. Internal restriction sites of the *Da FdIII* gene are indicated (*Pst*I and *Hin*cII). The RBS is shown in bold and the inverted-repeat structure (IR) is underlined, starting at nucleotide 326.

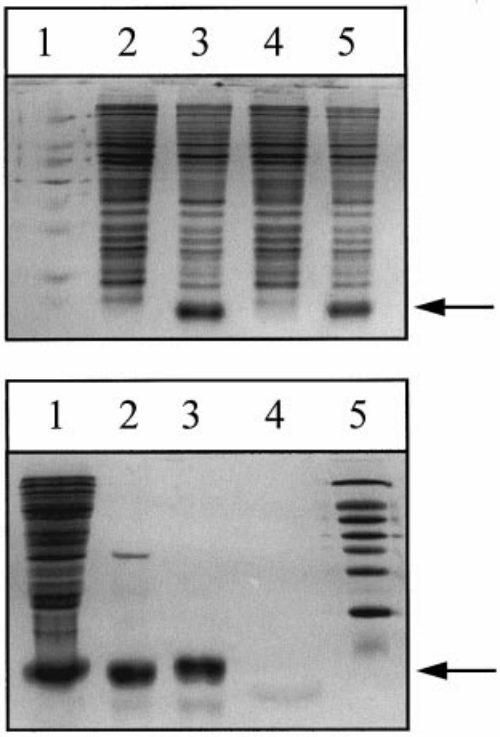

Figure 2 SDS/PAGE analyses of the expression and purification of ht *Da* FdIII

Upper panel: SDS/PAGE [20% (w/v) acrylamide] stained with Coomassie Blue. Lane 1, molecular-mass markers (66, 45, 36, 29, 24, 20, 14.2 and 6.5 kDa, respectively); lane 2, *E. coli* BL21(DE3) pLysS bearing plasmid pJB10 (synthetic gene), before induction; lane 3, same as lane 2, 3 h after IPTG induction; lane 4, *E. coli* BL21(DE3) pLysS bearing plasmid pJB11 (native gene), before induction; lane 5, same as lane 4, 3 h after induction. The arrow indicates the position of ht *Da* FdIII. Lower panel: SDS/PAGE [20% (w/v) acrylamide] stained with Coomassie Blue. Lane 1, supernatant after cell breakage; lane 2, ht *Da* FdIII-containing fraction after the affinity column; lane 3, purified ht *Da* FdIII after the subsequent Sephacryl S-100 column; lane 4, *Da* FdIII bearing the mutation $Asp^{14} \rightarrow Cys$; lane 5, molecular-mass markers (66, 45, 36, 29, 24, 20, 14.2 and 6.5 kDa, respectively). The arrow indicates the position of ht *Da* FdIII.

Apo-(ht *Da* FdIII) protein eluted from a nickel-affinity column and passed through a gel-filtration column was approx. 98% pure as judged by SDS/PAGE (Figure 2, lower panel). A contaminating band just below the main ht *Da* FdIII band could not be separated from ht *Da* FdIII. This contaminant may be the result of protein degradation, as it is not observed with freshly expressed ht *Da* FdIII, but only appears during the course of the purification, even in the presence of protease inhibitors. Approx. 30 mg of apo-(ht *Da* FdIII) was purified from 12 g of cells.

Electrospray MS of apo-(ht *Da* FdIII) solution (approx. 5 mg·ml^{-1} in 10 mM Tris/HCl, pH 7.6) were collected in the positive-ion mode. The apoprotein showed a mass of 7636.4 Da, close to the calculated mass of apo-(ht *Da* FdIII) of 7635.4 Da (results not shown), confirming the correct expression of ht *Da* FdIII in *E. coli*, with no post-translational processing of the polypeptide occurring.

Reconstitution of holo ht *Da* FdIII

Reconstitution of holo ht *Da* FdIII in the presence of a reducing agent, and with $FeCl_3$ and Na_2S as sources for iron and inorganic sulphide, respectively, was sluggish and complicated by the formation of a black precipitate that was difficult to remove [19]. Therefore NifS was used to mobilise sulphur from L-cysteine [26]. At low NifS: apo-(ht *Da* FdIII) ratios, cluster incorporation took place without FeS precipitation, but when the NifS to apoprotein ratio was increased a precipitate of FeS was formed. Excess reagents were removed chromatographically. DE 52 anion-exchange chromatography led to cluster loss, a black FeS precipitate remaining on the top of the column, but S-100-column chromatography did not lead to cluster loss.

Electrospray MS of reconstituted ht *Da* FdIII collected in either positive-ion mode or negative-ion mode only showed one strong band with a mass of 7636 Da corresponding to apo-(ht *Da* FdIII). Several small peaks constituting a broad band around 8000 Da were also observed, but these do not correspond to holo-(ht *Da* FdIII) which has a calculated mass 8282.8 Da. Ht *Da* FdIII bearing one $[4Fe\text{-}4S]^{2+/1+}$ cluster has a calculated mass of 7987.6 Da and so it is possible that the small peaks arise from this.

Absorption spectroscopy of reconstituted ht *Da* FdIII

The UV/visible absorption spectrum of reconstituted ht *Da* FdIII is typical of Fds with absorption maxima around 280 nm and 400 nm and a shoulder at 350 nm (Figure 3). The overall shape and intensity of the spectrum compares well with native *Da* FdIII. The major broad band lies at 408 nm, the absorption maximum of native *Da* FdIII. Typically A_{408}/A_{280} ratios (purity index) between 0.48 and 0.65 were obtained for similar sample preparations. Since the highest purity index is 0.78 [1] a range of 0.48–0.65 indicates that in all preparations some of the cluster binding sites were unoccupied. This is similar to our finding with rec *Da* FdIII which had a maximum purity index of 0.68 [19]. Reconstituted ht *Da* FdIII samples were stable when maintained anaerobically and no decrease of the purity index was observed upon ultrafiltration, in contrast to rec *Da* FdIII which rapidly lost cluster when concentrated [19].

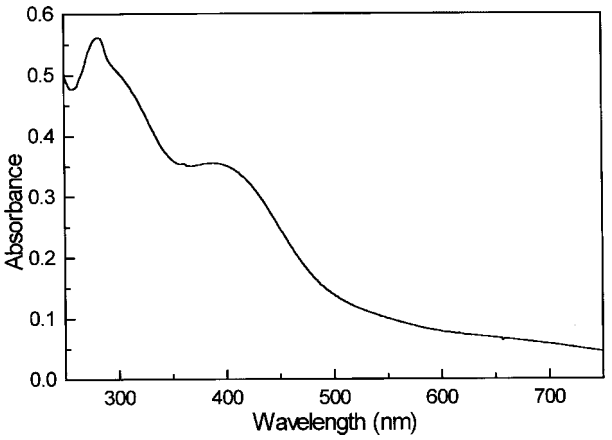

Figure 3 UV/visible spectrum of reconstituted ht *Da* FdIII

Reconstituted ht *Da* FdIII (120 μM in 20 mM Hepes, pH 7.4, 0.1 M NaCl, 100 μM EGTA) after S-100 chromatography and concentration. Purity index (A_{408}/A_{280}) = 0.63. The path length was 1 mm.

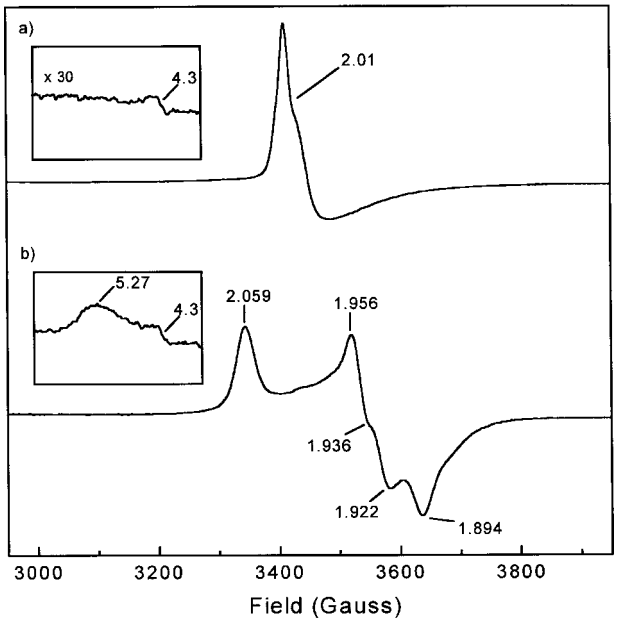

Figure 4 X-band EPR spectra of ht *Da* FdIII

(**a**) Protein concentration, 135 μM in 20 mM Hepes, pH 7.4, 0.1 M NaCl, 100 μM EGTA; purity index 0.63. Temperature, 6 K; gain, 2.0×10^4. The inset shows the g = 4.3 signal. Microwave power, 2 mW; microwave frequency, 9.64 GHz; modulation amplitude, 10 G. (**b**) Protein concentration, 180 μM in 20 mM Hepes, pH 7.4, 0.1 M NaCl; purity index, 0.63. The sample was reduced with excess dithionite. Temperature, 17 K; gain, 8.0×10^4. Microwave power, 2 mW; microwave frequency, 9.64 GHz; modulation amplitude, 10 G. The inset shows the g = 5.27 and 4.3 signals. Temperature, 12 K; gain, 1.25×10^5; microwave power, 83 mW; microwave frequency, 9.64 GHz; modulation amplitude, 10 G.

EPR spectroscopy of reconstituted ht *Da* FdIII

At a temperature of 10 K the EPR spectrum of 135 mM oxidized ht *Da* FdIII in the presence of 100 mM EGTA displays a slightly anisotropic signal at g = 2.01, comprising a low-field sharp positive peak with a shoulder, and a less-intense broad negative 'tail' at higher field (Figure 4a), typical of an oxidized $[3Fe\text{-}4S]^{1+}$ cluster [39]. On increasing the temperature the signal broadens, becoming difficult to observe at temperatures above 25 K. The signal shape and temperature behaviour are very similar to the EPR signal of oxidized native *Da* FdIII, which has been assigned to a $[3Fe\text{-}4S]^{1+}$ cluster with a spin ground state of S = 1/2 [2]. Double integration of the ht *Da* FdIII signal typically gave 0.8 ± 0.1 spins per ht *Da* FdIII. The EPR spectrum of oxidized ht *Da* FdIII also contains a weak signal at g = 4.3, typical of adventitious Fe(III) (Figure 4, inset). When EGTA was omitted from the sample only a weak signal could be observed at g = 2.01, suggesting that the $[3Fe\text{-}4S]^{1+}$ cluster had converted to a $[4Fe\text{-}4S]^{2+}$ cluster, which is EPR-silent. This contrasts with observations on native *Da* FdIII which displays [3Fe-4S]-cluster EPR signals in oxidized solutions devoid of chelator.

The EPR spectrum of dithionite-reduced ht *Da* FdIII consists of a rhombic signal centred at g = 1.94, with apparent g values of 2.059, 1.936 and 1.894 (Figure 4b). The signal is observed between 4 K and 35 K, although at the higher temperature some of its fine structure is lost. This signal is typical of a reduced $[4Fe\text{-}4S]^{1+}$ cluster with a spin ground state of S = 1/2 [3]. Double integration of the signal gave 0.9 ± 0.15 spin per ht *Da* FdIII consistent with one stable $[4Fe\text{-}4S]^{1+}$ cluster, as in native *Da* FdIII [3]. A small contribution from adventitiously-co-ordinated iron at g = 4.3 can also be seen (Figure 4b). At lower field the spectrum displays a signal with a g value of 5.27 (Figure 4b). The signal is weak at low power, but can be clearly visualized at high power and low temperatures (e.g. 80 mW and 12 K), and is not power saturated under these conditions (Figure 4b, inset). At higher temperatures the signal broadens and is difficult to measure. A similar signal has been observed in the EPR spectra of reduced native *Da* FdIII and rec *Da* FdIII, and was assigned to a $[4Fe\text{-}4S]^{1+}$ cluster with a spin ground state of S = 3/2, resulting from the reaction of the $[3Fe\text{-}4S]^{0}$ cluster with Fe(II) [3,19]. This [3Fe-4S] → [4Fe-4S]-cluster conversion on reduction of reconstituted ht *Da* FdIII was not prevented by the presence of EGTA, unlike native *Da* FdIII where the conversion is prevented by EGTA. Double integration of the g = 5.27 signal was not possible [3], but as the spectra do not display a low-field g = 12 signal, indicative of a reduced $[3Fe\text{-}4S]^{0}$ cluster with an S = 2 ground state [2], we conclude that the majority of the [3Fe-4S] clusters have been converted to [4Fe-4S] centres.

NMR spectroscopy of reconstituted ht *Da* FdIII

NMR spectra (1D) of apo- and reconstituted ht *Da* FdIII are very different (Figure 5), particularly in the appearance of 18 peaks shifted downfield of 9.6 p.p.m. in the spectrum of the reconstituted protein which indicate the presence of one or more paramagnetic iron-sulphur clusters. Based on studies of other Fds, these peaks are likely to arise from some of the βCH and αCH protons of the cluster-ligating cysteines. Analysis of inversion-recovery data (results not shown) enabled the T_1 times of 15 out of 18 peaks downfield of the diamagnetic region to be determined. With the exception of peaks 12, 15 and 16 these all had $T_1 < 10$ ms, indicative of enhanced proton relaxation. The linewidths at half-height of the well resolved, downfield-shifted peaks ranged between 180 and 490 Hz, typical of enhanced T_2 relaxation. The downfield signals of reconstituted ht *Da* FdIII were found to exhibit both anti-Curie (14 peaks) and Curie-temperature dependence (4 peaks). The 1D NMR data suggest that a di-cluster Fd has been reconstituted, as 18 strongly shifted peaks can be identified, of which the majority are fast relaxing and have temperature-dependent shifts. A maximum of 12 such peaks are expected for a [4Fe-4S] cluster and nine for a [3Fe-4S] cluster. Moreover, since Curie-temperature-dependent behaviour

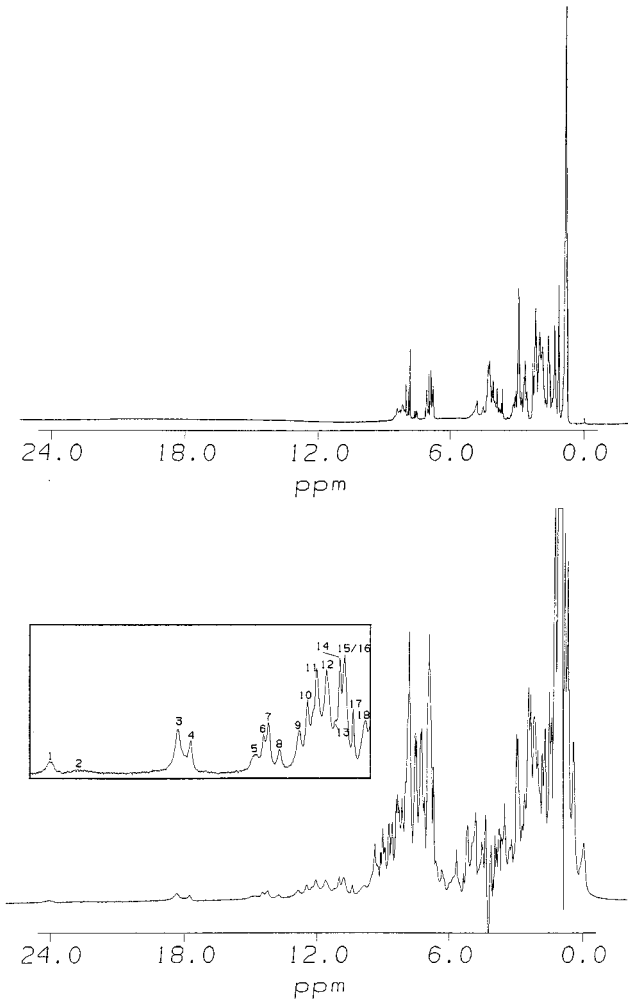

Figure 5 1D NMR spectra of oxidized ht *Da* FdIII

Upper panel: apo-(ht *Da* FdIII). Lower panel: holo-(ht *Da* FdIII). The spectra of both samples were recorded in 90% H_2O/10% ^2H_2O (by vol.), 100 mM phosphate buffer, pH 7.4, at 298 K. The peaks shifted downfield of 9.6 p.p.m. are shown in the inset of the lower panel, and are labelled 1–18.

has been reported only for oxidized Fds containing a $[3Fe\text{-}4S]^{1+}$ cluster, the Curie-temperature dependence observed for some of the downfield-shifted peaks of reconstituted ht *Da* FdIII indicates the presence of an oxidized 3Fe cluster. Although 7Fe Fds have not been extensively studied by ^1H NMR, two distinct chemical shift patterns have been observed [40]. The NMR data reported in the present study for ht *Da* FdIII are indicative of the shift pattern seen with the 7Fe *Desulfurolobus ambivalens* Fd [41], which appears to be connected with the cluster-binding sequence CysI-Xaa-Xaa-Asp/CysII-Xaa-Xaa-CysIII [40]. However, although similarities with the *D. ambivalens* Fd exist, *Da* FdIII exhibits two peculiarities; four Curie-temperature-dependent peaks and a larger number of hyperfine shifted peaks. These factors make the NMR characteristics of reconstituted ht *Da* FdIII unique, and it is possible that this results from the *Da* FdIII having a glutamate instead of a proline adjacent to CysIV in the binding motif of the transformable cluster [42,43].

The 1D NMR spectrum of apo-(ht *Da* FdIII) (Figure 5) is indicative of an unstructured protein with random-coil chemical shifts [44]. 2D ^1H-^1H TOCSY and NOESY spectra also suggest it is an unstructured protein (results not shown). The TOCSY spectra show a large number of overlapping NH-αCH cross-peaks between protons with chemical shifts of $\delta \approx 8.0$–8.6 p.p.m. and $\delta \approx 3.8$–4.7 p.p.m. indicating that the resonances have not been shifted significantly from their values in small peptides. The NOESY spectrum was also devoid of the NOE correlations expected for secondary and tertiary structural elements [44]. NMR spectra of reconstituted ht *Da* FdIII indicate that in contrast to the apoprotein it contains secondary structural elements. This is evident, for example, from the increased dispersion of NH resonances and from NOE correlations in the NH-NH region of 2D NOESY spectra (results not shown). These features can be readily obwserved even though the sample of reconstituted ht *Da* FdIII contains up to 40% of apo-(ht *Da* FdIII) as judged by the purity index.

The aromatic region of the NMR spectrum is of particular interest because this is the location of signals of the histidine side chain resonances of the ht. In addition to the six histidine residues, ht *Da* FdIII contains two tyrosine residues and two residues each of asparagine and glutamine, whose NH_2 groups have resonances in the aromatic region. Resonances of four of the histidines of the ht have been identified in 1D- and 2D-TOCSY spectra (Figure 6) of apo-(ht *Da* FdIII) but corresponding resonances have not been identified in the spectra of holo-(ht *Da* FdIII), despite resonances from tyrosine residues and side chain NH_2 groups being observed in both apo- and holo-(ht *Da* FdIII). A possible explanation for this result is that the ht has bound some Fe(III) that broadens the histidine resonances.

Electrochemistry

The cyclic voltammogram of a protein film of ht *Da* FdIII (prepared from a solution containing 0.1 mM EGTA) (Figure 7a) shows three signals (pairs of oxidation and reduction peaks) labelled A′, B′ and C′ according to previous studies on wild-type *Da* FdIII [2,11]. By analogy with native *Da* FdIII and other 7Fe Fds, the three signals are assigned to the respective redox couples $[3Fe\text{-}4S]^{1+/0}$, $[4Fe\text{-}4S]^{2+/1+}$ and $[3Fe\text{-}4S]^{0/2-}$ [2]. Signal A′ shows a reduction potential $E^{0'} = -150 \pm 10$ mV, and a half-height peak width of ≈ 90 mV, close to the theoretical value (84 mV at 2 °C) for a Nernstian one-electron process. Signal B′, associated with $[4Fe\text{-}4S]^{2+/1+}$, shows a reduction potential of $E^{0'} = -390 \pm 10$ mV and half-height peak widths of ≈ 107 mV. In each case the modest peak separations are consistent with reasonably fast electron transfer reactions. Signal C′ is of higher intensity, and the slightly sharper oxidation peak has a half-height width of 79 mV; $E^{0'} = -733 \pm 10$ mV. The combination of signal A′ and the novel low-potential two-electron signal C′ is a characteristic of [3Fe-4S] clusters when studied by protein-film voltammetry, and, as described below, provides the means to test transformation activities. Reduction potentials $E^{0'}$ (± 10 mV) of the three couples are very similar to those observed for native *Da* FdIII, which have been reported previously as $E^{0'} = -140$ mV for A′, $E^{0'} = -390$ mV for B′ and $E^{0'} = -720$ mV for C′ (at pH 7.15, 0 °C) [45]. Provided polymyxin was present in the electrolyte, protein-film voltammograms of ht *Da* FdIII were relatively stable; the potential could be cycled repeatedly with no apparent signal intensity loss over periods of at least 30 min.

The pH dependence of the three redox couples measured over the pH range 5–8 was essentially identical to that of native *Da* FdIII [12]; i.e. signals A′ and B′ only vary slightly with pH, whereas signal C′ shows strong pH-dependent behaviour, consistent with the two-electron reduction of $[3Fe\text{-}4S]^0$ being accompanied by the net binding of two H^+ [45,46].

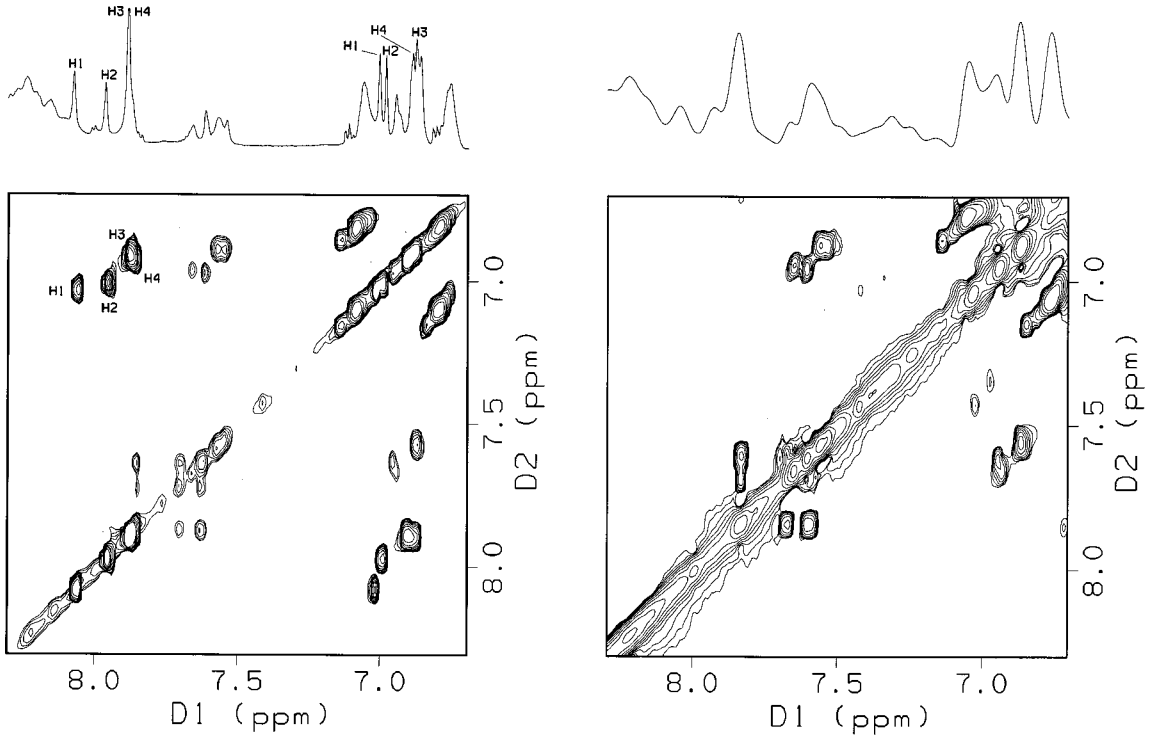

Figure 6 Aromatic region of the 50ms 2D NMR TOCSY spectra of ht *Da* FdIII

Left-hand panel: spectrum of apo-(ht *Da* FdIII) at 288 K in 90% H_2O/10% ^2H_2O (by vol.), 100 mM phosphate, pH 7.4. The 4 cross-peaks assigned to histidine residues of the ht are designated H1, H2, H3 and H4. The corresponding singlets on the 1D trace (above) have also been labelled. Right-hand panel: the corresponding region of the 50 ms ^1H-^1H TOCSY spectrum of holo-(ht *Da* FdIII) under the same conditions. The peaks labelled H1, H2, H3 and H4 are no longer present.

The reactivity of the [3Fe-4S] cluster of ht *Da* FdIII was tested by transferring protein films to electrolyte solutions supplemented with Fe(II) or Zn(II). Figure 7(b) shows the transformation [3Fe-4S] → [Fe:3Fe-4S] occurring in ht *Da* FdIII after transferring a film-coated electrode to a 200 mM Fe(II)-containing solution, and poising the potential at −500 mV for 60 s before cycling. Signals A′ and C′ disappeared simultaneously with the appearance of a new signal (D′), having a potential close to that of B′ so that B′ and D′ are superimposed. The original voltammogram was restored (Figure 7c) upon returning the film-coated electrode to the metal-free electrolyte and poising the potential at 350 mV before cycling. By analogy with studies on native *Da* FdIII, the new signal D′ is assigned to the transformed [4Fe-4S]$^{2+/1+}$ cluster with $E^{0'} \approx -390$ mV, which loses the labile iron upon oxidative degradation [12]. Similar results were obtained with 200 mM Zn(II)-supplemented electrolyte solutions, leading to the reversible formation of a [Zn:3Fe-4S] species, with $D'_{Zn(II)}$ signal estimated at $E^{0'} \approx -517 \pm 10$ mV (results not shown). Thus the reversible transformation of the [3Fe-4S]$^{1+/0}$ cluster with Fe(II) and Zn(II) was accomplished in protein films, similar to observations with native *Da* FdIII showing that ht *Da* FdIII is very similar to wild-type *Da* FdIII in its film voltammetry properties.

DISCUSSION

The main purpose of the preparation of ht *Da* FdIII was to obtain a substitute protein for native *Da* FdIII, which is only expressed in very low amounts. Previously a recombinant form of *Da* FdIII had been prepared [19]. Reconstituted rec *Da* FdIII carried iron-sulphur clusters with electronic and magnetic properties similar to those of native *Da* FdIII but cluster stability was low, as shown by degradation upon mild treatment such as concentration in ultrafiltration units or chromatography. To determine whether such instability could result from an incorrect amino-acid sequence, from difficulties with the chemical method of cluster incorporation, or from incorrect folding during reconstitution that may have trapped the holoprotein in a less-favourable fold, the DNA sequence of the *Da* FdIII gene was determined. This has confirmed that the synthetic gene for rec *Da* FdIII was based on the correct amino-acid sequence and that the polypeptide expressed in *E. coli* has the same composition as wild-type *Da* FdIII. Thus the low stability of rec *Da* FdIII does not result from an incorrect amino-acid sequence [19]. The stability problems with rec *Da* FdIII may relate to the chemical insertion of iron-sulphur clusters through the *in vitro* addition of $FeCl_3$ and Na_2S to the polypeptide in the presence of DTT. Although successful reconstitution procedures have been reported for various Fds (e.g. for 8Fe *Clostridium pasteurianum* Fd [47]), *in vitro* cluster incorporation is not a direct substitute for the complex cluster-insertion and folding machinery of the bacterial cell. *In vitro* cluster-insertion methods are often imperfect; for example the supposed 7Fe *Rhodobacter capsulatus* FdII and *Azotobacter vinelandii* FdI were both reported to contain two [4Fe-4S] clusters after reconstitution [48,49]. From the EPR and electrochemical data presented in the present study, ht *Da* FdIII is very similar to native *Da* FdIII in the composition of the reconstituted iron-sulphur centres, and the NMR data are consistent with thse results in indicating the presence of both [3Fe-4S] and [4Fe-4S] clusters. Thus the reconstitution procedure

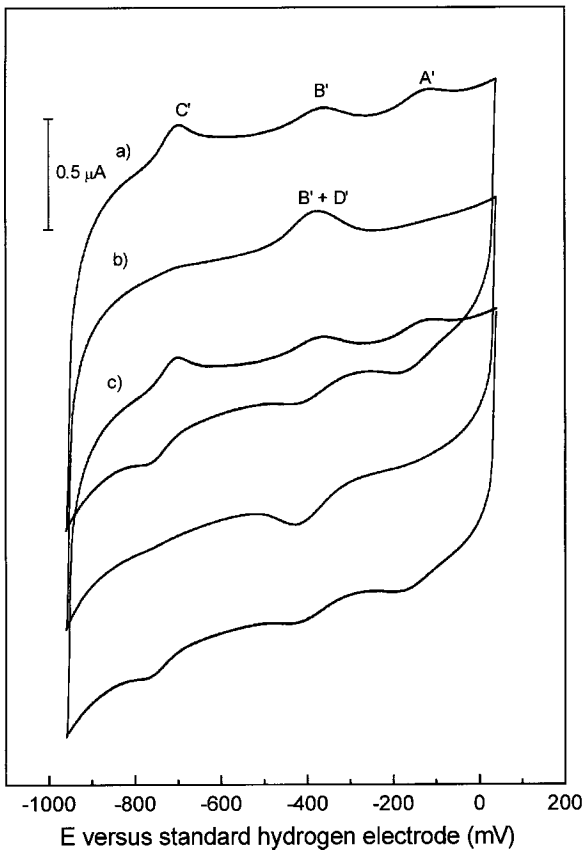

Figure 7 Cyclic voltammograms of films of ht *Da* FdIII, showing Fe(II) uptake and release

(**a**) A film was prepared from a 120 μM ht *Da* FdIII solution (purity index 0.63) in 20 mM Hepes, pH 7.4, 0.1 M NaCl, 100 μM EGTA and containing 0.2 mg ml^{-1} polymyxin. The electrolyte solution consisted of 20 mM Hepes, pH 7.4, 0.1 M NaCl, 100 μM EGTA and 0.2 mg ml^{-1} polymyxin. The scan rate was 50 mV s^{-1}. The temperature was 2 °C. The sets of waves are labelled A′, B′ and C′. D1 and D2 are the chemical shifts in the first and second dimension, respectively. (**b**) The electrode and film were transferred to an electrolyte solution also containing 200 μM Fe(II). The solution was stirred and poised for 60 s at −500 mV prior to scanning. The set of waves associated with the $[Fe:3Fe\text{-}4S]^{2+/1+}$ couple is labelled D′. (**c**) The electrode and film were returned to the original non-metal-containing electrolyte solution. The electrode was poised at +350 mV before the scan was recorded.

with NifS worked well, though full cluster incorporation was not attained with any preparation.

The UV/visible and EPR spectroscopic results and the electrochemical data indicate that the iron-sulphur clusters were largely unaffected by the presence of the ht. However, the histidine residues of the tag are not detected by NMR when the metal clusters are present. It is unlikely that resonances of these residues are broadened by the cluster. An alternative possibility is that excess Fe(III) is present, possibly binding to the ht. A g = 4.3 signal is seen in the EPR spectrum that could arise from this source. If the Fe(III) were in fast exchange between different protein molecules sub-stoichiometric amounts could cause the NMR effects observed. For example, in studies of high-spin Fe(III) complexes binding to proteins, less than one Fe(III) per 100 molecules has been seen to cause substantial broadening [50]. The presence of excess Fe(III) may contribute to the reduced stability of ht *Da* FdIII compared to the native protein by promoting cluster destruction.

Future work will report on the properties of proteins modified by site-directed mutation of residues around the [3Fe-4S] cluster binding site.

We thank Dr. E. Claude Hatchikian (CNRS, Marseille, France) for providing *D. africanus* cells and Dr. Dennis R. Dean (Virginia Polytechnic Institute, Blacksburg, VA, U.S.A.) for sending plasmid pDB551. Dr. Richard Jones is thanked for fermentations, Mr. Rick Evans-Gowing for mass spectroscopy and Ms. Elaine Patrick (Centre for Metalloprotein Spectroscopy and Biology, University of East Anglia, Norwich, U.K.) for the construction of plasmids pJB12 and pJB13. We thank the EPSRC and BBSRC for their support of the University of East Anglia, Centre for Metalloprotein Spectroscopy and Biology via their Biomolecular Sciences Panel, and The Wellcome Trust for their support of the University of East Anglia NMR facility.

REFERENCES

1 Bovier-Lapierre, G., Bruschi, M., Bonicel, J. and Hatchikian, E. C. (1987) Biochim. Biophys. Acta **913**, 20–26
2 Armstrong, F. A., George, S. J., Cammack, R., Hatchikian, E. C. and Thomson, A. J. (1989) Biochem. J. **264**, 265–273
3 George, S. J., Armstrong, F. A., Hatchikian, E. C. and Thomson, A. J. (1989) Biochem. J. **264**, 275–284
4 Cammack, R. (1992) Adv. Inorg. Chem. **38**, 281–322
5 Asso, M., Mbarki, O., Guigliarelli, B., Yagi, T. and Bertrand, P. (1995) Biochem. Biophys. Res. Commun. **211**, 198–204
6 Moura, J. J. G., Xavier, A. V., Hatchikian, E. G. and LeGall, J. (1978) FEBS Lett. **89**, 177–179
7 Aono, S., Bertini, I., Cowan, J. A., Luchinat, C., Rosato, A. and Viezzoli, M. S. (1996) J. Biol. Inorg. Chem. **1**, 523–528
8 Minami, Y., Wakabayashi, S., Wada, K., Matsubara, H., Kerscher, L. and Oesterkelt, D. (1985) J. Biochem. (Tokyo) **97**, 745–753
9 Wakabayashi, S., Fujimoto, N., Wada, K., Matsubara, H., Kerscher, L. and Oesterkelt, D. (1983) FEBS Lett. **162**, 21–24
10 Bentrop, D., Bertini, I., Luchinat, C., Mendes, J., Piccioli, M. and Teixeira, M. (1997) Eur. J. Biochem. **236**, 92–99
11 Butt, J. N., Niles, J., Armstrong, F. A., Breton, J. and Thomson, A. J. (1994) Nat. Struct. Biol. **1**, 427–433
12 Butt, J. N., Fawcett, S. E. J., Breton, J., Thomson, A. J. and Armstrong, F. A. (1997) J. Am. Chem. Soc. **119**, 9729–9737
13 Carney, M. J., Papaefthymiou, G. C., Spartalian, K. R. B. and Holm, R. H. (1988) J. Am. Chem. Soc. **110**, 6084–6095
14 Lindahl, P. A., Day, E. P., Kent, T. A., Orme-Johnson, W. H. and Münk, E. (1985) J. Biol. Chem. **260**, 11160–11173
15 Moura, I., Moura, J. J. G., Münk, E., Papaefthymiou, V. and LeGall, J. (1986) J. Am. Chem. Soc. **108**, 349–351
16 Moreno, C., Macedo, A. L., Moura, I., LeGall, J. and Moura, J. J. G. (1994) J. Inorg. Biochem. **53**, 219–234
17 Finnegan, M. G., Conover, R. C., Park, J.-B., Zhou, Z. H., Adams, M. W. W. and Johnson, M. K. (1995) Inorg. Chem. **34**, 5358–5389
18 Staples, C. R., Dhawn, I. K., Finnegan, M. G., Dwinell, D. A., Zhou, Z. H., Huang, H., Verhagen, M. F. J. M., Adams, M. W. W. and Johnson, M. K. (1997) Inorg. Chem. **36**, 5740–5749
19 Busch, J. L. H., Breton, J. L. J., Bartlett, B. M., James, R., Hatchikian, E. C. and Thomson, A. J. (1996) Biochem. J. **314**, 63–71
20 Grosjean, H. and Fiers, W. (1982) Gene **18**, 199–209
21 Sambrook, J., Fritsch, E. F. and Maniatis, T. (1989) Molecular Cloning: A Laboratory Manual, 2nd edn., Cold Spring Harbor Laboratory Press, Plainview, NY
22 Hatchikian, E. C. and Bruschi, M. (1981) Biochim. Biophys. Acta **634**, 41–51
23 Gerhardt, P. (1994) Methods for General and Molecular Bacteriology, American Society of Microbiology, ASM Press, Washington D.C
24 Inouye, M., Arnheim, N. and Sternglanz, R. (1973) J. Biol. Chem. **248**, 7247–7252
25 Laemmli, U. K. (1970) Nature (London) **227**, 680–685
26 Zheng, L., White, R. H., Cash, V. L. and Dean, D. R. (1994) Biochemistry **33**, 4714–4720
27 Aasa, R. and Vänngård, T. (1975) J. Magn. Reson. **19**, 308–315
28 Inubushi, T. and Becker, E. D. (1983) J. Magn. Reson. **51**, 128–133
29 Vold, R. L., Waugh, J. S., Klein, M. P. and Phelps, D. E. (1968) J. Chem. Phys. **48**, 3831–3832
30 Bax, A., Davis, D. G. and Sarkar, S. K. (1985) J. Magn. Reson. **63**, 230–234
31 Macura, S. and Ernst, R. R. (1980) Mol. Phys. **41**, 95
32 Griesinger, C., Otting, G., Wüthrich, K. and Ernst, R. R. (1988) J. Am. Chem. Soc. **110**, 7870–7872
33 Bax, A. and Davies, D. G. (1985) J. Magn. Reson. **65**, 355–360

34 Piotto, M., Saudek, V. and Sklenár, V. (1992) J. Biol. NMR. **2**, 661–665
35 Marion, D., Ikura, M., Tschudin, R. and Bax, A. (1989) J. Magn. Reson. **85**, 393–399
36 Armstrong, F. A., Butt, J. N. and Sucheta, A. (1993) Methods Enzymol. **227**, 479–500
37 Stokkermans, J. P. W. G., Pierik, A. J., Wolbert, R. B. G., Hagen, W. R., van Dongen, W. M. A. M. and Veeger, C. (1992) Eur. J. Biochem. **208**, 435–442
38 Lewin, B. (1996) Genes V (1996) Oxford University Press, Oxford
39 Beinert, H. and Thomson, A. J. (1983) Arch. Biochem. Biophys. **222**, 333–361
40 Bertini, I., Dikiy, A., Luchinat, C., Macinai, R., Viezzoli, M. S. and Vincenzini, M. (1997) Biochemistry **36**, 3570–3579
41 Bentrop, D., Bertini, I., Luchinat, C., Mendes, J., Piccioli, M. and Teixeira, M. (1996) Eur. J. Biochem. **236**, 92–99
42 Gaillard, J., Quinkal, I. and Moulis, J.-M. (1993) Biochemistry **32**, 9881–9887
43 Quinkal, J., Davasse, V., Gaillard, J. and Moulis, J. M. (1994) Protein Eng. **5**, 681–687
44 Wüthrich, K. (1986) NMR of Proteins and Nucleic Acids, Wiley, New York
45 Armstrong, F. A., Butt, J. N., George, S. J., Hatchikian, E. C. and Thomson, A. J. (1989) FEBS Lett. **259**, 15–18
46 Breton, J., Duff, J. L., Butt, J. N., Armstrong, F. A., George, S. J., Pétillot, Y., Forest, E., Schäfer, G. and Thomson, A. J. (1995) Eur. J. Biochem. **233**, 937–946
47 Moulis, J.-M. and Meyer, J. (1982) Biochemistry **21**, 4762–4771
48 Armengaud, J., Gaillard, J., Forest, E. and Jouanneau, Y. (1995) Eur. J. Biochem. **231**, 396–404
49 Morgan, T. V., Stephens, P. J., Burgess, B. K. and Stout, C. D. (1984) FEBS Lett. **167**, 137–141
50 Moore, G. R., Eley, C. G. S. and Williams, G. (1983) Adv. Inorg. Bioinorg. Mech. **3**, 1–96

Received 26 May 1999/ 8 October 1999; accepted 2 December 1999